Solid State Communications, Vol. 85, No. 7, pp. 553-559, 1993.
Printed in Great Britain.

0038-1098/93$6.00+.00
Pergamon Press Ltd

MAGNETIC STRUCTURE OF Ho_2BaNiO_5

E. García–Matres, J. Rodríguez–Carvajal† and J.L. Martínez††

Institut Laue–Langevin, BP 156, F–38042, Grenoble Cedex, FRANCE.

A. Salinas–Sánchez and R. Sáez-Puche

Dep. Química Inorgánica, Fac. Ciencias Químicas, Universidad Complutense, E–28040 Madrid, SPAIN.

(Received 26August 1992, by Paul Burlet, in revised form 13 November 1992)

The magnetic behaviour of Ho_2BaNiO_5 has been characterized by means of neutron powder diffraction from 1.5 K to Room Temperature (RT). This orthorhombic compound (S.G. *Immm*, a≈3.764 Å, b≈5.761 Å, c≈11.336 Å) is structurally characterized by the presence of NiO_6 octahedra forming chains along the a–axis. Three Dimensional Antiferromagnetic ordering (3D–AF) is established for both Ho and Ni sublattices at T_N≈53 K. The propagation vector of the magnetic structure is **k**=[1/2 0 1/2]. At 1.5 K the magnetic moments lie in the ac-plane and have values of 9.0 μ_B (Ho) and 1.4 μ_B (Ni), the moment of Ho^{3+} is nearly paralell to the c-axis and the smallest angle of the Ni-moment direction with the c-axis is 26°. The strong magnetic moment reduction of Ni^{2+} cations is probably due to a combination of low–dimensional quantum effects and covalency. A smooth re-orientation, governed by the magnetic anisotropy of Ho^{3+}, seems to occurs below and very close to T_N; i.e. the Ni moments rotate from nearly paralell to the a-axis toward the c-axis following the Ho moments. The thermal evolution of the magnetic structure from T_N until 1.5 K is studied in detail.

INTRODUCTION

The R_2BaNiO_5 (R=Rare earth or Y) oxides present many interesting structural and magnetic properties. They belong to the orthorhombic system, S.G *Immm*, having approximate cell parameters around a≈3.8 Å, b≈5.8 Å, c≈11.3 Å These oxides are characterized by the presence of one-dimensional (1D) chains of NiO_6 octahedra along the a–axis. The octahedra are strongly distorted with a very short Ni–O_{apical} distance (≈1.88 Å), and a longer Ni–O_{basal} distance (≈2.18 Å). Moreover the basal angle (≈80°) is also smaller than the 90° of a regular octahedra [1–8]. From the structural point of view it is interesting to point out that the compounds with the heaviest rare earth ions (Tm, Yb and Lu) present a second type of structure. This second polymorph is characterized by NiO_5 pyramidal coordination of the Ni^{2+} ions [9, 10]. Why only the compounds with smallest rare earth ions are dimorphic is still an open question.

From the magnetic point of view these oxides are also appealing: due to the structural characteristics, i.e. the absent of direct oxygen links between chains, these compounds are perfect candidates to study low dimensional magnetic properties. In fact Y_2BaNiO_5 presents one-dimensional Antiferromagnetic (1D–AF) correlations as shown by the magnetic susceptibility data [5, 6]. Moreover, neutron diffraction shows the absence of 3D–AF ordering above 1.5 K. The exchange constant of the 1D–AF Ni chain, as obtained from the magnetic susceptibility, is J/k=322 K (≈28 meV) [5]. The magnetic coupling between chains is very weak as evidenced by the lack of 3D–AF ordering. In the case of the rest of the family (Nd–Tm), the magnetic coupling mediated by the paramagnetic rare earth ions is strong enough for coupling the chains and a 3D–AF ordering is obtained at temperatures between 30 K and 60 K. At T_N both sublattices (Ni and R) become simultaneously 3D–AF ordered. From the microscopic point of view the best characterized compounds are Er_2BaNiO_5 and Y_2BaNiO_5 [8]. In the former case the ordering temperature is T_N≈33 K, with a propagation vector **k**=[1/2 0 1/2] and the magnetic moments at 4 K are 1.54 μ_B and 7.9 μ_B for Ni and Er, respectively. The moments of both sublattices point along the a–axis (chain direction), with a small canting along the z direction. The value of T_N is different from temperature of the maximum, observed by different authors, in the magnetic susceptibility. For instance T_{Max}≈15 K in Er_2BaNiO_5 [3,7]. This compound presents also two metamagnetic transitions at 4 K, their nature and mechanism being not yet studied by microscopic techniques [7]. The rest of compounds of this family have been characterized by bulk magnetic susceptibility. In particular a maximum in the susceptibility is observed for Ho_2BaNiO_5 at 33 K, as well as two metamagnetic transitions at 33 kOe and 23 kOe [7]. The aim of this article is to characterize the microscopic magnetic behaviour of Ho_2BaNiO_5 in comparison with the isomorphous Er_2BaNiO_5.

† Present address: Laboratoire Léon Brillouin (CEA-CNRS), Centre d'Etudes de Saclay, 91191 Gif sur Yvette Cedex, FRANCE.

†† Present address: Instituto de Ciencia de Materiales de Madrid (CSIC). Fac. Ciencias (C–4). Universidad Autónoma de Madrid. E–28049 Madrid. SPAIN.

EXPERIMENTAL

Ho_2BaNiO_5 oxide was prepared as polycrystalline samples by solid state reaction from stoichiometric high purity oxides Ho_2O_3 (99.999%) $BaCO_3$ (Reactive for Analysis grade) and NiO (99.999%) by heating in air at 1200° C for 48 hours, with several interruptions for grinding.

The neutron diffraction data were obtained in the medium–resolution high–flux D1B powder diffractometer at the High Flux Reactor of the Institut Laue Langevin (Grenoble, France). The diffractometer is equipped with a Position Sensitive Detector (PSD) covering an angular range of 80°(2θ) and working at λ=2.52 Å. The PSD is composed of 400 sensitive elements separated by 0.2°(2θ) . A He cryostat was used in the temperature range between 1.5 K and RT.

All the data were analyzed with the Rietveld method using the program FULLPROF [11]. The simplicity of the structure (only three free position-parameters) allows to obtain reliable parameters in spite of the low resolution instrument D1B. We have translated the origin of the unit cell, with respect that given in Ref. [8], by a vector [1/2 0 0]; thus the Ni ions are at (0, 0, 0). The background was fitted to a polynomial function. The magnetic form factors were calculated from Ref. 12 for Ni^{2+} and Ho^{3+}. In the later case the dipolar approximation was used.

EXPERIMENTAL RESULTS

The crystallographic structure of Ho_2BaNiO_5 has been characterized in detail in a previous work [10]. As stated above, this compound is orthorhombic with space group *Immm* and the Wyckoff positions occupied by atoms are collected in Table I. At low temperature the peaks from the

TABLE I

Structural parameters and reliability factors of the Rietvel refinement of Ho_2BaNiO_5 at RT and 1.5 K. Data at RT from Ref. 10 and those of 1.5 K correspond to a full magnetic and crystal structure refinement, the magnetic data are collected in Table IV.

	RT	1.5 K
Lattice parameters (Å)		
a	3.76370(4)	3.75453(7)
b	5.76101(8)	5.7319(4)
c	11.3357(1)	11.2715(4)
Volume ($Å^3$)	245.79	242.57
Ho (1/2 0 z)		
z	0.2028(1)	0.2025(4)
B($Å^2$)	0.41(2)	-
Ba (1/2 1/2 0)		
B($Å^2$)	1.02(5)	-
Ni (0 0 0)		
B($Å^2$)	0.65(3)	-
O(1) (0 y z)		
y	0.2410(3)	0.2414(16)
z	0.1488(1)	0.1495(6)
B($Å^2$)	0.56(4)	-
O(2) (1/2 0 0)		
B(Å2)	0.74(3)	-
Overall B($Å^2$)	-	0.5
Number of reflections	158	19
Reliability factors (%)		
R_{wp}	5.07	6.86
R_{exp}	2.64	1.29
χ^2	3.69	28.2
R_B	4.71	3.14

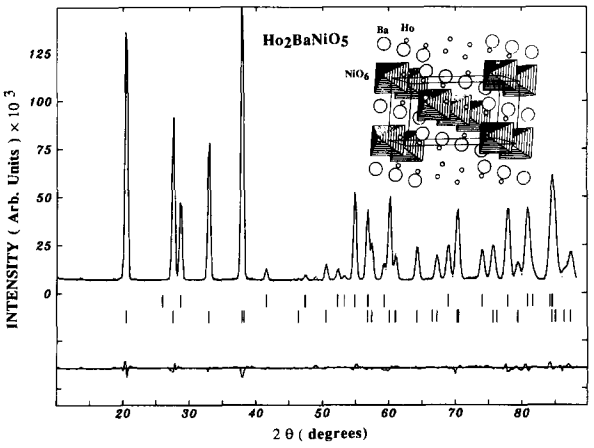

Fig. 1. Neutron diffraction pattern of Ho_2BaNiO_5 at 1.5K. The solid line is the calculated profile and vertical marks correspond to the position of the allowed Bragg reflections for the crystallographic (first row) and magnetic structures (second row). The difference curve is plotted at the bottom of the figure. The inset shows the crystal structure of this family of compounds with the NiO_6 octahedra chains.

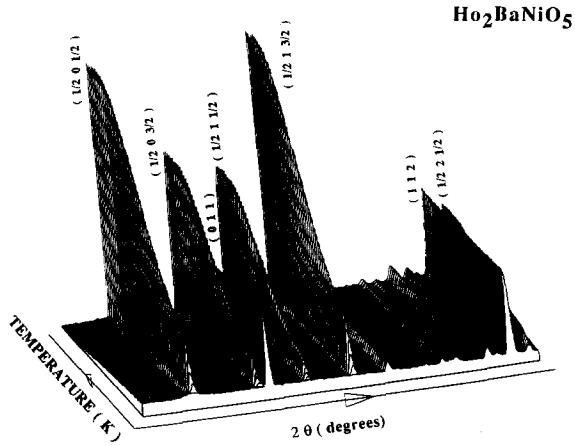

Fig. 2. Temperature dependence (between 1.5 K and 65 K) of the diffraction patterns of Ho_2BaNiO_5. Angular range from 15° to 58°(2Θ), λ =2.52 Å.

3D–AF ordering are easily observed (Fig. 1). The diffraction patterns in a 2θ range from 15 to 58 degrees, and temperatures from 1.5 K to 60 K, are presented in Fig. 2. The main features observed in the figure are: the strong intensity of the AF Bragg peaks and the corresponding reduction of the background associated with the ordering of the paramagnetic ions. Both facts are related to the strong magnetic moment associated with the Ho^{3+} ions. It is also interesting to point out the relative high ordering temperature ($T_N \approx 53$ K) observed for Ho_2BaNiO_5. Rare earths in oxides usually order at much lower temperatures.

The temperature dependence of the lattice parameters is presented in Fig. 3. It is interesting to point out that due to the fixed position of the D1B detector the relative accuracy in the cell parameters is high, although the absolute values may depend on systematic errors (zeros of motors, λ calibration...). The data represented in Fig. 3 show that the thermal expansion in this narrow temperature range (1.5 K to 65 K) is anisotropic. The *a*-axis is almost constant or with a slightly negative thermal expansion coefficient, whereas *b* and *c*-axes show a clear positive linear dependence on temperature, with a change in the slope at ≈33 K. It is also worth remarking that the *a*–axis (chain direction) shows a tiny discontinuity (an expansion on going from high to low temperatures) at $T_N \approx 53$ K, certainly related with the 3D–AF ordering and the accompanying striction effects.

ANALYSIS OF RESULTS AND DISCUSSION

Structural refinements

The main structural details at RT, as obtained from high resolution powder neutron diffraction, has been shown in a previous report [10]. Here we shall concentrate in the temperature dependence of this structure. In the above mentioned work we were interested in the variation of this unit as a function of the rare earth ionic size ("chemical pressure" effect). As a matter of fact the volume of the NiO_6 octahedra varies linearly with the size of the rare earth ions, indicating that the chemical pressure is nearly hydrostatic. The temperature dependence of the main distances and angles in the NiO_6 octahedra is presented in Fig. 4. Obviously, the distance Ni–O(2) along the chain follows closely the variation of the *a*-axis. The distance Ni–O(1) in the basal plane is almost constant showing a tiny change in the slope around 33 K. Another important

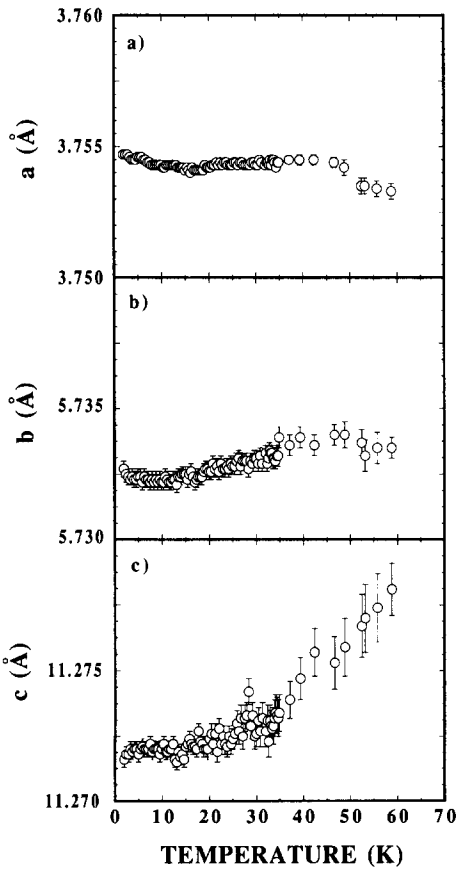

Fig. 3. Variation of the lattice parameters *a*, *b* and *c* with temperature.

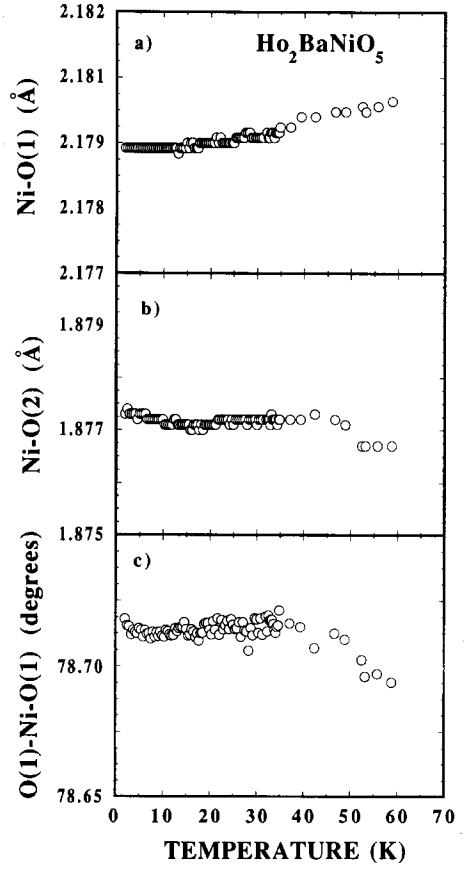

Fig. 4. Axial (a) and equatorial (b) distances of the NiO_6 octahedra, and the angle O(1)–Ni–O(1) (c) *vs.* temperature for Ho_2BaNiO_5.

point is that the angle O(1)–Ni–O(1) in the basal plane presents a clear dependence on temperature from T_N to 33 K, being almost constant from 33 K to 1.5 K. By contrast the Ba–O(2) and Ho–O(2) distances are almost constant, within the error bars, from 1.5 K to 70 K (not shown). The main structural parameters at RT and 1.5 K are presented in Table I.

Group Theory Analysis

Below T_N≈53 K all the observed Bragg peaks were indexed within a commensurate lattice related to the crystallographic one (*Immm*) by a propagation vector **k**=[1/2 0 1/2] (the components are referred to the reciprocal vectors of the conventional unit cell). The symmetry operations of the high temperature space group ($T>T_N$), which keep invariant the propagation vector or transforms it into an equivalent vector, differing by an arbitrary vector of the reciprocal lattice, form the wave vector group G_k. In our case, we have $G_{k/T}=\{E, m_y, 2_y, i\}$, where T is the invariant translation subgroup.

The irreducible representations of the entire space group G are specified by the star of the wave vector {**k**}, which is a set of non–equivalent wave vectors obtained by the application of all the symmetry elements of the point group G_0. In our case the star has two arms, constituted by the propagation vectors $\mathbf{k}_1$=[1/2 0 1/2] and $\mathbf{k}_2$=[1/2 0 -1/2]. However, within the hypothesis of constant modulus of magnetic moments (*spins*), the magnetic structure should be described with a single propagation vector.

Because G_k is a symmorphic group the irreducible representations are obtained from those of its point group G_{0k}. Table II gives the character of the irreducible representations Γ^v of G_{0k}.

In the case of Ho_2BaNiO_5, the Ho sublattices are generated by two atom sites at 1: (1/2 0 z) and 2: (1/2 0 -z) in a primitive unit cell, with magnetic moment components $S_{i\alpha}$, being i=1, 2 and α=x, y, z. The rest Ho atoms of the conventional unit cell are related by the centering translation [1/2 1/2 1/2]. The magnetic moment in positions outside from the reference cell are calculated from those at the primitive cell, $\mathbf{S}_o$, by the expression,

$$\mathbf{S}_t = \mathbf{S}_o \exp [2 \pi i \mathbf{k} \mathbf{t}]$$

being **t** the Bravais translation connecting the two positions. We define the following two magnetic modes for the Ho atoms in a primitive cell:

$$\mathbf{F} = \mathbf{S}_1 + \mathbf{S}_2 \qquad \mathbf{A} = \mathbf{S}_1 - \mathbf{S}_2$$

From the transformation properties of the spin vectors we generate a reducible representation Γ of G_k. The four transformation matrices of the symmetry operations {E, m_y, 2_y, i} in the space of $S_{i\alpha}$ components, have 6 x 6 dimension and their traces are (6, -2, 0, 0).

In the case of Ni, only one atom located at (0, 0, 0) with magnetic components S_α (α=x, y, z) generate the whole sublattice. The dimension of the representative matrices is 3 x 3, and their traces are (3, -1, -1, 3) for the same symmetry operations. By the application of standard formulae, the irreducible representations contained in Γ(Ho) and Γ(Ni) are:

$$\Gamma(Ho)=A_g + 2B_g + B_u + 2A_u$$

$$\Gamma(Ni)=A_g + 2B_g$$

Table III represents the basis vectors of both the Ho and Ni sublattices. Following the Bertaut method, only vectors belonging to the same representation of both sites (Ho and Ni) may be coupled [13, 14], in first approximation.

In a previous paper [8], there are some typing error in the ordering of the character of the Γ(Ho) and Γ(Ni) representations. Moreover, the use of the time reversal operator is not necessary. However, the representations in Table II are identical to those used in Ref. 8, as well as the magnetic structures described by the basis vectors. The only important remark is that the new definition of the origin implies a change in the "label" of the basis functions: the old A's become F's and vice versa (compare our Table III with Table III of Ref. 8).

TABLE II

Irreducible representations of the wave vector group G_{0k} (*2/m*), with **k**=[1/2 0 1/2] of G=*Immm*.

	E	m_y	2_y	i
A_g	1	1	1	1
B_g	1	-1	-1	1
A_u	1	-1	1	-1
B_u	1	1	-1	-1

TABLE III

Basis vector for the Ho and Ni sublattices.

	Ho			Ni		
	x	y	z	x	y	z
$\Gamma^1 A_g$	-	F_y	-	-	S_y	-
$\Gamma^2 B_g$	F_x	-	F_z	S_x	-	S_z
$\Gamma^3 A_u$	A_x	-	A_z	-	-	-
$\Gamma^4 B_u$	-	A_y	-	-	-	-

Magnetic structure refinements

As in the case of the Er compound the best fit of the experimental data is obtained for the B_g representation, therefore the full magnetic structure has four free parameters as indicated by the numerical coefficients of B_g in Γ's. In the Ho case the relationship between the two magnetic moments of the primitive cell is $S_{2x}=S_{1x}$, $S_{2y}=S_{1y}=0$, and $S_{2z}=S_{1z}$. In the case of the Ni sublattice the two basis vectors are directly the x and z components of the magnetic moment. This means that the Ni and Ho magnetic moments are restricted to the *a–c* plane.

In Fig. 1 is shown the observed and calculated patterns at 1.5 K. Table IV shows a summary of the magnetic moments for Ho^{3+} and Ni^{2+} at 1.5 K and those of the Er-compound for comparison. The magnetic moments are written in the cartesian components allowed by the magnetic structure (S_x, 0, S_z) as well as in spherical coordinates (μ, θ, ϕ). The main results are that the magnetic moments of Ho are nearly aligned along the *c*-axis, i.e. perpendicular to the chains of NiO_6 octahedra, whereas the direction of the Ni moments forms an angle with the *c*-axis of 26°. The refined parameter θ=154°, corresponds to the angle of the magnetic moment with the *positive* direction [001]. The value of the magnetic moment for Ho is 9.0 μ_B, close to the expected value for the free ion Ho^{3+} (10 μ_B). In the case of Ni the magnetic moment is 1.4 μ_B. This value is lower than that expected for Ni^{2+} (2 μ_B). Even in nearly 2D-systems like La_2NiO_4 with Ni^{2+} in octahedral coordination, the saturation moment is close to 1.5 μ_B, being explained this reduction by covalency effects and quantum spin fluctuations in 2D [15]. In the present case 1.4 μ_B represents a stronger reduction probably due to the strong covalency related to the very unusual short apical distance of 1.88 Å.

It is interesting to compare these results with those obtained in the isomorphous Er_2BaNiO_5 [8]. The magnetic structure of the two compounds is the same, but the magnetic moments are almost parallel to the chains (*a*-axis) in the case of Er and perpendicular to the chains (along the *c*-axis) in the case of Ho. This reflects the different direction of the anisotropy of the two rare earth ions. A representation, by means of the program MAG3D [16], of the Ho_2BaNiO_5 magnetic structure compared with that of Er_2BaNiO_5 is shown in Fig. 5.

TABLE IV

Magnetic moments for Ho^{3+} and Ni^{2+} in Ho_2BaNiO_5 at 1.5 K, in cartesian and spherical coordinates ($R_{Mag.}$=1.6%). The values in italic correspond to the Er_2BaNiO_5 compound with the new origin.

	Ho	Er	Ni	
$S_X(\mu_B)$	0.12(5)	*7.89(4)*	0.58(9)	*-1.40(4)*
$S_Z(\mu_B)$	9.06(4)	*0.25(4)*	1.26(4)	*-0.64(7)*
$\mu(\mu_B)$	9.06(5)	*7.89(4)*	1.41(5)	*1.54(5)*
θ(°)	0.7(3)	*88.2(3)*	154(4)	*-115(2)*

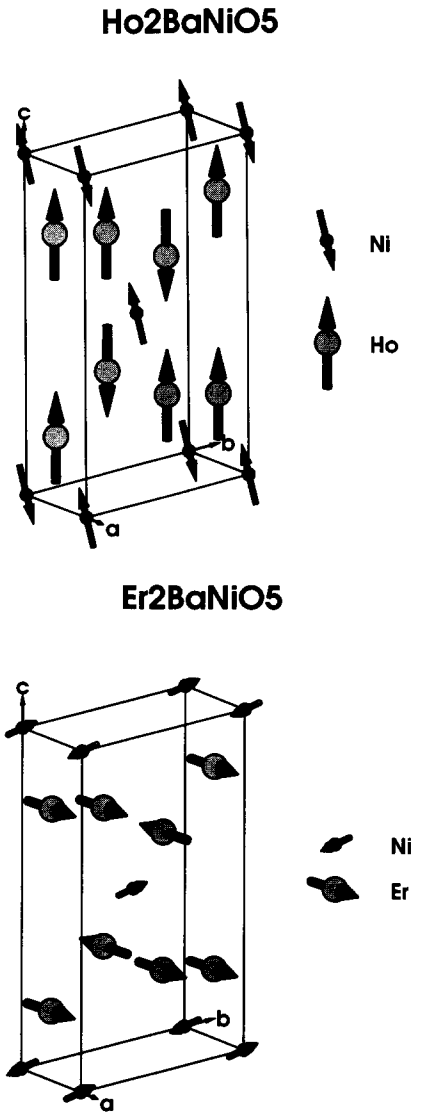

Fig. 5. Representation of the Ho_2BaNiO_5 and Er_2BaNiO_5 magnetic structures at 1.5 K. Only one crystallographic unit cell is shown.

Temperature dependence of the magnetic structure

Let us now discuss the thermal evolution of the magnetic moments in Ho_2BaNiO_5. Fig. 6(a) shows the temperature dependence of the Ho^{3+} magnetic moment and the rather high (≈53 K) Néel temperature. In Fig. 6(b) it is depicted the variation of the θ angle with temperature. The error bars around the ordering temperature become important due to the small ordered moment. The main

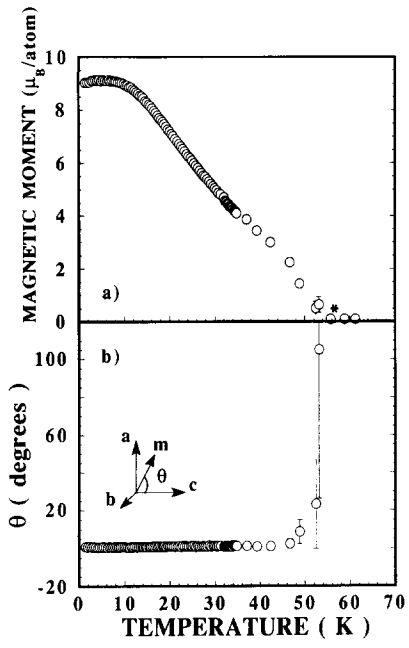

Fig. 6. Temperature dependence of the Ho^{3+} magnetic moment (a), and θ angle, as defined in the inset (b).

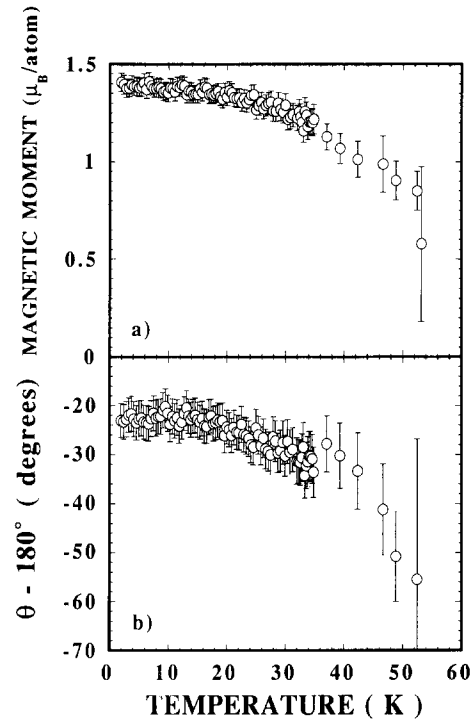

Fig. 7. Temperature dependence of (a) Ni^{2+} magnetic moment, and (b) θ–180° angle, θ is defined in the inset of the previous figure.

feature is that the value of the magnetic moment is close to the free ion value (10 μ_B), and is almost fully aligned parallel to the *c*–axis (θ≈0°). This indicates that the single ion anisotropy of Ho^{3+} in these compounds is clearly directed along the *c*–axis. It is also interesting to point out the shape of the Ho magnetic moment *vs.* temperature curve. First, there is an almost linear behaviour from T_N≈53 K to the saturation temperature around 12 K. Second, inside this temperature range there is a clear change in the slope around 33 K.

In Fig. 7(a) is represented the magnetic moment of Ni^{2+} *vs.* temperature showing that the ordering temperature is the same than that of the Ho sublattice. The magnetic moment reach a saturation value of 1.4 μ_B at 12 K. In Fig. 7(b) is shown the temperature dependence of the θ–180° angle of the reference Ni(0,0,0) atom. Our results suggest that close to T_N the Ni sublattice starts to be ordered with the magnetic moments pointing mainly along the NiO_6 chain. A similar direction is observed in Er_2BaNiO_5 for the whole temperature range.

As in the case of the Y-compound, Ho_2BaNiO_5 should present strong 1D–AF correlations well above RT. It is quite probable that these correlations have a fluctuating character in time, so no static 1D ordering exist. The 1D–AF correlations are very difficult to be observed from magnetic susceptibility due to the important paramagnetic moment from the Ho ions. In neutron diffraction quasi-static 1D–AF ordering does not produce any Bragg peak, but a small jump in the background signal at a 2θ value corresponding to the 1D–AF periodicity along the chain. If the energy of the 1D-AF fluctuations is out of the energy window of the diffraction experiment nothing is seen. Near, but above, T_N quasi-static short-range ordering is observed. The diffuse scattering up to T_N + 10K is likely due to the Ni–Ho interactions, which are responsible of the coupling between different chains, establishing the short-range ordering.

Just below, but close to T_N, the Ni moments start to rotate toward the *c*–axis, forced by the combination of the increasing ordered moment on the Ho site, the exchange $J_{Ni\text{-}Ho}$ and the anisotropy of the Ho^{3+} due to crystal field. Around 33 K, the Ni moment is mostly aligned along the *c*–axis with a small component parallel to the *a*–axis.

It is interesting to point out that at 33 K there is a clear change in the slope for the Ho magnetic moment and a maximum is observed in the magnetic susceptibility. This family of compounds (R_2BaNiO_5) presents maxima in the magnetic susceptibility, which are always at much lower temperatures that the 3D–AF ordering temperatures (T_N) observed by neutron diffraction. For instance, in Er_2BaNiO_5 the temperature of the maximum is T_{Max}≈16 K and T_N≈33 K; for Ho_2BaNiO_5 T_{Max}≈33 K and T_N≈53 K [17]. This effect could be related to the dependence on applied external magnetic field of the measured magnetic susceptibility (5 kOe to 10 kOe), and the zero field data in the case of neutron diffraction, but it is also important noticing that in low-dimensional magnetic systems a

maximum in magnetic susceptibility is not directly related to 3D–AF ordering process.

Concluding remarks

It is interesting to remark the close connection between the magnetic and crystal structures. Magneto-elastic effects seems to appear at T_N: a discontinuity in the *a*-axis is observed. After the rotation of the Ni magnetic moments toward the *c*–axis, at 33 K, a change in the slope is observed in the *c*–axis, as well as in the octahedra O(1)–Ni–O(1) angle.

After Cherpuko *et al.* [7], the R_2BaNiO_5 (R=Nd, Gd, Dy, Ho, Er) oxides present two metamagnetic transitions at 4.2 K for magnetic fields between 15 kOe to 180 kOe. In the case of Ho_2BaNiO_5 these metamagnetic transitions are observed at 23 kOe and 33 kOe. However no good quality data are available yet, with the corresponding values of the magnetization associated with each metamagnetic transition. Nevertheless, these transitions will be probably associated with changes in the propagation vector of the magnetic structure.

Finally, an important point should be considered. There is some indications, supported by semi-empirical calculations, that Ni^{2+} in flattened octahedra must be in a diamagnetic low-spin state ($t^6_{2g}\ d^2_{x2-y2}\ d^0_{z2}$) [18]. However, our experimental results on this family of compounds show clearly the existence of a well defined magnetic moment in the Ni sites. The origin of the contradiction should be in the assumption, in the above mentioned calculations [18], of a negligible intra-atomic Coulomb electronic correlation. What our data suggest is that the splitting between d_{x2-y2} and d_{z2} energy levels due to crystal field, is not enough to overcome the intra-atomic exchange energy, and the Hund's rule is still working.

REFERENCES

1. ST. Schiffler and HK. Müller–Buschbaum, Z. Anorg. Allg. Chem. **540/541**, 243 (1986). See also, H. Mevs and HK. Müller–Buschbaum, J. Less Common Metals **152**, 139 (1989).
2. J. Amador, E. Gutierrez-Puebla, M.A. Monge, I. Rasines, J.A. Campá, J.M. Gómez de Salazar and C. Ruiz-Valero, Sol. St. Ionics **32/33**, 123 (1989).
3. J. Amador, E. Gutierrez-Puebla, M.A. Monge, I. Rasines, C. Ruiz-Valero, F. Fernández, R. Sáez-Puche and J.A. Campá, Phys. Rev. **B42**, 7918 (1990).
4. D.J. Buttrey, J.D. Sullivan and A.L. Rheingold, J. Sol. St. Chem. **88**, 291 (1990).
5. R. Sáez-Puche, J.M. Coronado, C.L. Otero-Díaz and J.M. Martín-Llorente, J. Sol. St. Chem. **93**, 461 (1991).
6. R. Sáez-Puche, J.M. Martín-Llorente and J.M. Coronado, J. Less Common Metals **175**, 131 (1991).
7. G.G. Chepurko, Z.A. Kazei, D.A. Kudrjavtsev, R.Z. Levitin, B.V. Mill, M.N. Popova and V.V. Snegirev, Phys. Lett. **A157**, 81 (1991).
8. J.A. Alonso, J. Amador, J.L. Martínez, I. Rasines, J. Rodríguez-Carvajal and R. Sáez-Puche, Sol. St. Commun. **76**, 467 (1990).
9. A. Salinas-Sánchez, R. Sáez-Puche, J. Rodríguez-Carvajal and J.L. Martínez, Sol. St. Commun. **78**, 481 (1991).
10. E. García-Matres, J.L. Martínez, J. Rodríguez-Carvajal, J.A. Alonso, A. Salinas-Sánchez and R. Sáez-Puche, J. Sol. St. Chem (Submitted).
11. J. Rodríguez-Carvajal, "FULLPROF: A Program for Rietveld Refinement and Pattern Matching Analysis", Abstracts of the Satellite Meeting on Powder Diffraction of the XV Congress of the International Union of Crystallography, p. 127, Toulouse (France), 1990.
12. P.J. Brown, Institut Laue-Langevin Report SP88BR5016 (1988).
13. E.F. Bertaut, Acta Cryst. **A24**, 217 (1968). See also, E.F. Bertaut, Ann. Phys. **A24**, 217 (1968).
14. J. Rossat–Mignod in "Methods of Experimental Physics", Vol 52 part C (1987). Academic Press, New York.
15. J. Rodríguez-Carvajal, M.T. Fernández-Díaz and J.L. Martínez, J. Phys.: Condens. Matt. **3**, 3215 (1991), and references therein.
16. P.J. Brown, ILL (unpublished).
17. R. Sáez-Puche, A. Salinas-Sánchez, I. Rasines, Mat. Chem. Phys. **31**, 151 (1992).
18. J.K. Burdett and J.F. Mitchell, J. Am. Chem. Soc. **112**, 6571 (1990)